EAGE

CONFERENCE & EXHIBITION
NEAR SURFACE GEOSCIENCE'23

Fault zone identification using seismic noise autocorrelations at a prospective geothermal site in Singapore

Karen Lythgoe[1], Yunyue Elita Li[2], Shengji Wei[3], Jonathan Poh[4], Hendrik Tjiawi[4]

1. *School of Geosciences, University of Edinburgh, Scotland*
2. *Earth, Atmospheric, and Planetary Sciences, Purdue University, USA*
3. *Earth Observatory of Singapore, Nanyang Technological University, Singapore*
4. *Energy Research Institute, Nanyang Technological University, Singapore*

Introduction

Faults play an important role in transporting fluids through Earth's crust, and can therefore be a key factor in determining the success of geothermal projects. Hot springs in Singapore indicate the existence of hot water that could potentially be exploited in a low-enthalpy geothermal development. Faults within the granitic bedrock are thought to be a key pathway to transport the hot water from depth to surface.

A borehole is currently being drilled at a site near to surface hot springs in Singapore. The borehole aims to assess rock properties and temperatures at depths up to 1.5 km. Lack of open space in highly urban Singapore, necessitates that the drilling location is constrained to a small grassy site in a residential area (Figure 1). The site geology is expected to be granite overlain with a thin sedimentary cover. The granite is known to be heavily faulted, based on regional geology and evidenced by fault zone rocks intercepted in several geotechnical boreholes. Extensive above ground development in Singapore means that any surface geomorphological features of faulting have been eliminated.

We acquired passive seismic data at the prospective geothermal site to investigate the subsurface and identify any fault zones. We chose to use a passive survey since it is non-invasive, environmentally friendly, has low labour requirements and is simple to obtain required permissions. Specifically, we use the autocorrelation of seismic noise. The autocorrelation function simulates a virtual source located at the same location as the geophone, which is equivalent to a zero-offset Green's function, containing the reflection response beneath a receiver. Therefore, by autocorrelating continuous records of ground motion from noise sources, Earth's reflection response can be obtained (Claerbout 1968).

Single station autocorrelations differ from two-station interferometry in that it retrieves the reflection response beneath a station. The Green's function retrieved by two-station interferometry is often dominated by surface waves, which do not easily image the sharp impedance changes we are aiming to detect. Additionally, using autocorrelations places no requirement on instruments being deployed at the same time, so measurements can be infilled at a later date. Noise autocorrelations have been successfully used to image basin and crustal scale structures (e.g. Clayton 2020), although they have so far been less well used in near-surface geophysics, with a few notable exceptions (e.g. Zhang et al 2021).

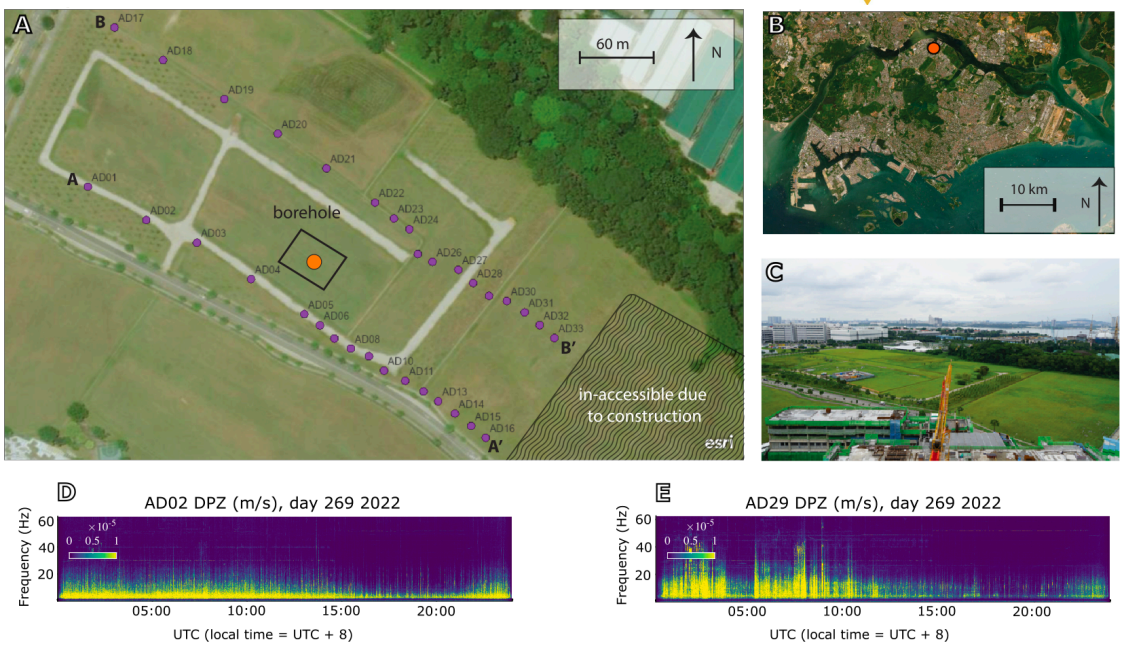

***Figure 1**. Drilling site (~400m by 200m) and locations of seismic nodes (A, B, C). Spectrograms for Monday 26th Sept (julian day 269) for station AD02 (D) and AD29 (E).*

Data and Methods

We deployed 33 three-component seismic nodes for 5-weeks, beginning on 24th September 2022. Two 2-D profiles were acquired along the longest edge of the area and designed to intercept a suspected fault zone striking ~N-S, based on a previous resistivity survey and regional faulting. Node spacing ranged from 15m to 40m (Figure 1), with denser spacing above the suspected fault zone. Spectrograms indicate extensive anthropogenic noise, occurring at frequencies from ~2-20 Hz, with greatest amplitude in the day (~8am to 6pm local time, Figure 1). Stations to the SE have the largest amplitude of high-frequency noise, which is likely from a construction site in this direction. Low frequencies (< 2Hz) in Singapore generally originate from the coastline (Nilot et al 2020, Li et al 2019).

Continuous data is processed by first removing the instrument response and down-sampling. Temporal normalisation is then applied, which removes coherent signals such as impulsive arrivals but retains phase information. Autocorrelations are computed in the frequency domain, with only the causal part retained. Processing is performed on data in one-hour windows. All resulting autocorrelations for each station are stacked to produce the final autocorrelation for the station.

Autocorrelations are equivalent to subsurface reflectivity convolved with a source function (Claerbout 1968). To isolate the reflectivity, we minimise the effect of the source by removing an estimate of the source time function which manifests as the zero-lag spike (and side lobes). We estimate the source time function as the mean of all autocorrelation functions along each profile. Following Clayton (2020), the source function is removed from the autocorrelation functions by subtraction, since it is more stable than deconvolution. The residual autocorrelation functions after subtracting the mean, are therefore an estimate of the subsurface reflectivity below each station, equivalent to a zero-offset section. Imaging using autocorrelations is also referred to as interferometric/seismic daylight imaging (Schuster et al 2004). For daylight imaging, we apply spectral whitening to the continuous data before autocorrelation, which acts to reduce the impact of the source by balancing the frequency spectrum.

Results

Figure 2 shows the mean power spectral density (PSD) along each profile. More high frequency energy (>~10 Hz) is recorded at stations to the SE towards the construction site. If the medium is homogeneously attenuative, the PSD is expected to decrease smoothly as distance increases from the noise source. While this is true for frequencies >~10 Hz, for low frequencies however, we find that there is a shift in the peak of the PSD function, from ~5 Hz to the SE, to ~3Hz to the NW, hinting at a change in medium properties along the line. We further analyse the spectral content for all three components in Figure 3 by looking at the autocorrelations in the frequency domain. The change in peak frequency along the profiles is clearly seen, particularly for the horizontal components. The peak frequency is related to the bedrock depth, suggesting deeper bedrock to the NW.

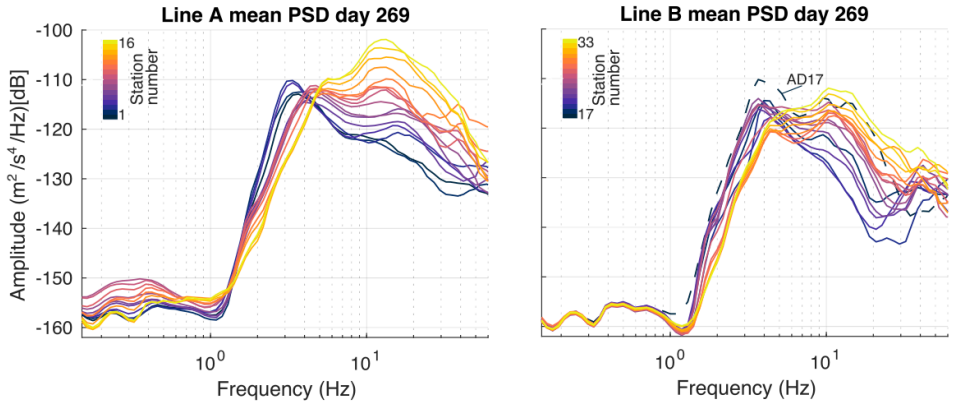

Figure 2. *Vertical component PSD computed for 30 minute windows on 26th Sept.*

The residual autocorrelations (after removing the estimated source function), show a high coherency between neighbouring stations and between the profiles (Figure 4). Investigating different frequency bands, the highest coherency is found between approximately 3-8 Hz for both profiles, although coherent signals can be found from ~1-16 Hz. The first arriving high amplitude peak is likely the reflection from the sediment-bedrock interface, with a two-way time consistent with the expected bedrock reflection based on results from the borehole (Figure 5). There is a pronounced change in reflectivity along the line. At the north-west, the first arrival is high amplitude arriving at ~0.13 s TWT. Moving to the south-east, the first arrival becomes very weak, and then arrives at high amplitude again at ~0.06 s TWT. The change in reflectivity occurs at ~200 m along each line and matches with the change in peak frequency, likely indicating the location of a fault zone, which we have interpreted in Figure 5. Based on the correlation between the two profiles, the fault is trending NNW-SSE. The borehole intersected a thick (~10 m apparent thickness) well-developed fault rock (composed of completely fractured and altered granite in a clay matrix) at ~550 m depth. Assuming expected subsurface velocities, this fault rock would occur at ~0.3 s TWT at the borehole, which is approximately consistent with the interpreted fault zone (Figure 5).

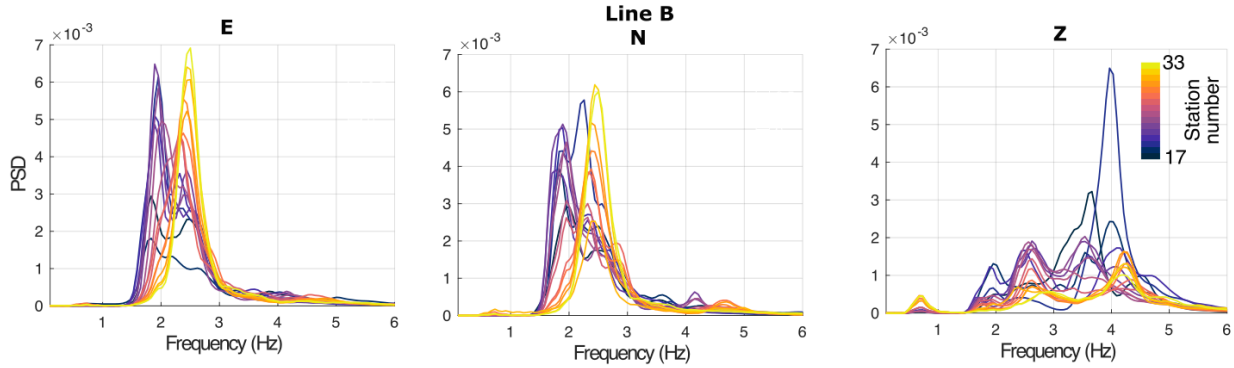

Figure 3 *Power spectral density (PSD) of autocorrelations for stations in line B.*

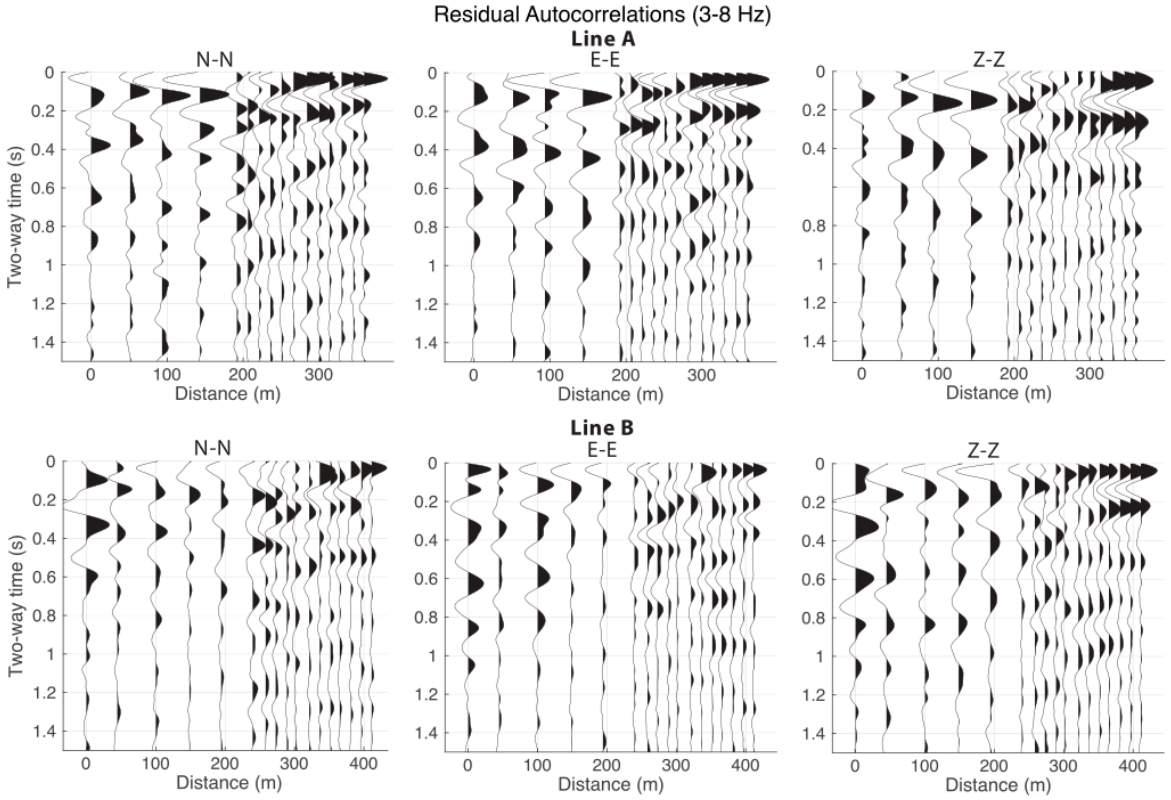

Figure 4. *Residual autocorrelations (~reflectivity) for all components at lines A (top) and B (bottom).*

Discussion

The shift in peak frequency indicates a change in bedrock depth approximately halfway along the profiles, at approximately the same location that the autocorrelation residuals indicates an offset in reflectors (Figure 5). The interferometric daylight imaging approach shows high coherency between stations and consistency with results from the borehole. However there are a number of limitations in the interferometric daylight imaging approach. The first relates to uncertainties in the source function. We simply estimate the source function as the mean across all traces, and so horizontal structure may also be included in the source estimation and removed from the resulting reflectivity. The source function should also be deconvolved, whereas in our approach, we do a straightforward subtraction. Additional uncertainties relate to the presence of multiples. The source of ambient noise is generally located at the surface, which is a deviation from the original theory of Claerbout (1968) which assumes a plane wave arriving from below. The one-sided illumination resulting from only surface sources may cause the retrieval of multiples or ghosts (e.g. Draganov et al., 2004, Schuster et al., 2004). Several studies have shown consistency between autocorrelation images based on ambient noise and teleseismic earthquake coda (travelling vertically

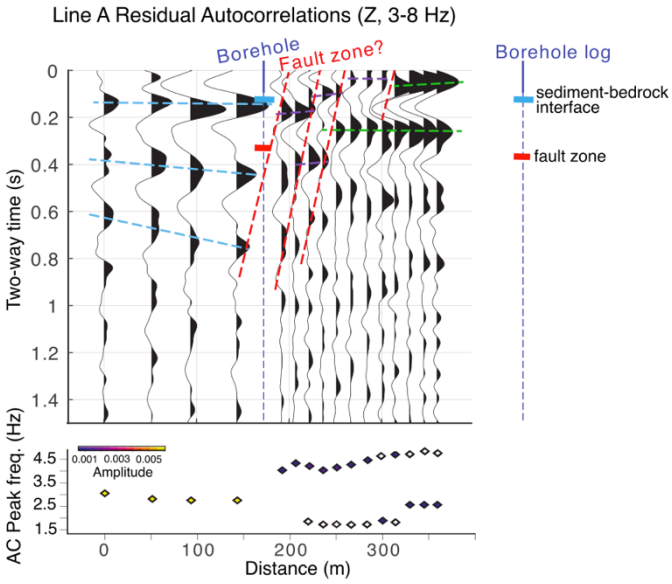

Figure 5 *Approximately interpreted vertical component residual autocorrelations and peak frequency of autocorrelations (AC) for line A.*

upwards), however these images are generally for frequencies < ~3 Hz, where noise sources may be more distributed. The two-way travel time of later arrivals in our autocorrelation reflectivity are not consistent with simple surface-related multiples, although we cannot rule out the presence of more complicated multiples.

Conclusions

We use autocorrelation of seismic noise to locate a fault zone in the near-surface at a prospective geothermal site. Specifically, we use interferometric daylight imaging, in addition to analysing the peak frequency of the autocorrelation functions, to investigate near-surface structures. Our results are broadly consistent with other geophysical methods and with core from the borehole. The approach is straightforward in terms of data acquisition and processing, although we caution that there are limitations, primarily related to the interpretation of later signals that may be contaminated by multiples and the suspected breakdown in the theoretical assumptions underpinning the method.

References

Claerbout, J. F. (1968). Synthesis of a layered medium from its acoustic transmission response. *Geophysics*, *33*(2), 264-269.

Clayton, R. (2020). Imaging the Subsurface with Ambient Noise Autocorrelations. *Seismological Research Letters*, 91 (2A): 930–935.

Draganov, D., Wapenaar, K., & Thorbecke, J. (2004). Passive seismic imaging in the presence of white noise sources. *The Leading Edge*, *23*(9), 889-892.

Li, Y., E., Zhang, Y., Nilot, E., Ku, T. (2019) Passive seismic methods for shallow and deep bedrock detection in Singapore. *Fifth International Conference on Engineering Geophysics* 176-180.

Nilot, E., Li, Y. E., Lythgoe, K. (2020) Bedrock detection based on seismic interferometry using ambient noise in Singapore. *SEG Technical Program Expanded Abstracts* 3577-3581.

Schuster, G. T., Yu, J., Sheng, J., & Rickett, J. (2004). Interferometric/daylight seismic imaging. *Geophysical Journal International*, *157*(2), 838-852.

Zhang, Y., Li, Y. E., & Ku, T. (2021). Soil/rock interface profiling using a new passive seismic survey: Autocorrelation seismic interferometry. *Tunnelling and Underground Space Technology*, *115*, 104045.